Journal of Sound and Vibration (1999) **224**(4), 733–756
Article No. jsvi.1999.2208, available online at http://www.idealibrary.com on IDEAL®

VIBRATION ANALYSIS OF AN INDUCTION MOTOR

C. WANG AND J. C. S. LAI

Acoustics and Vibration Unit, University College, The University of New South Wales Australian Defence Force Academy, Canberra, ACT 2600, *Australia*

(*Received* 14 *January* 1998 *and in final form* 28 *January* 1999)

With the advent of power electronics, variable speed induction motors are finding increasing use in industries because of their low cost and potential savings in energy consumption. However, the acoustic noise emitted by the motor increases due to switching harmonics introduced by the electronic inverters. Consequently, the vibro-acoustic behaviour of the motor structure has attracted more attention. In this paper, considerations given to modelling the vibration behaviour of a 2·2 kW induction motor are discussed. By comparing the calculated natural frequencies and the mode shapes with the results obtained from experimental modal testing, the effects of the teeth of the stator, windings, outer casing, slots, end-shields and support on the overall vibration behaviour are analyzed. The results show that when modelling the vibration behaviour of a motor structure, the laminated stator should be treated as an orthotropic structure, and the teeth of the stator could be neglected. As the outer casing, end-shields and the support all affect the vibration properties of the whole structure, these substructures should be incorporated in the model to improve the accuracy.

1. INTRODUCTION

Inverter-driven induction motors are finding increasing use in industrial and domestic applications because these drives are generally more efficient and offer potential savings in energy consumption and/or because the applications require continuously variable speeds. However, it has been found that some variable speed drives produce unacceptably high acoustic noise levels and the noise spectra vary with the speed of the drives. According to previous investigations [1, 2], this is primarily because some harmonics of the magnetic force introduced by the inverter coincide with some of the modes of the mechanical structure. Obviously, to control this noise, there are two strategies. One is to design inverters, of which the undesirable harmonics are eliminated. The other is to change the acoustic and vibration behaviour of the motor structure. Up till now, most studies have been mainly concentrated on developing pulse width modulation (PWM) inverters, such as random modulation [3] and programmed modulation [4–6], etc., to reduce the effects of the harmonics or to avoid the coincidences. Relatively few papers have dealt with the vibro-acoustic problems of motor structures. However, as pointed out by Timar and Lai [7], and Timar *et al.* [8], because the vibro-acoustic

0022-460X/99/290733 + 24 $30.00/0

behaviour of the motor structure usually determines the lowest limit of the noise or vibration levels that can be achieved by improving the inverter, the vibro-acoustic generation mechanism of motor structures, particularly those of variable speed induction motors, needs to be investigated. In fact, it is not difficult to realize that a deep understanding of the vibro-acoustic behaviour of inverter-driven motors will be of great benefit not only to implement retrofit noise control measures economically, but also for engineers to incorporate "quite" strategies in the design phase of motors.

The vibration analysis of a structure normally involves experimental testing and theoretical analysis. While there are numerous studies [9–13] on the modal analysis of a motor structure, they are primarily concerned with finding modes of the whole structure. Discussions about the effects of each part of the motor structure on the overall behaviour, and the influence of testing conditions on the results have not been documented.

The first effort to model and analyze the vibration behaviour of a motor structure theoretically can be traced back to the beginning of this century. Den Hartog [14] studied a method for calculating the natural frequencies of a stator of the single-ring type. Later, Jordan *et al.* [15] introduced in their calculations the effects of shear and rotary inertia, and the results were shown to be acceptable for medium-power machines. Pavlovsky [16] treated the stator as a single thick shell loaded with teeth and winding. Verma and Girgis [17] investigated the effects of core thickness and core lengths. As most stators of motors are of the double-shell type, consisting of an outer frame and an inner stator core, Erdelyi [18] considered a model of two thin shells joined by key bars, but the results were close to the measured data only when the ratio of the radial thickness of the core to the mean radius of the core was less than 0·2. To improve this model, Ellison and Yang [19] calculated the natural frequencies of a stator consisting of a thin frame and a thick laminated core loaded with teeth and windings, solidly coupled by key bars. However, none of these methods has been proved to be effective for real motor structures. This is because, in these analyses, the real motor structure has been greatly simplified but it has been found in practice and confirmed by experiments [2] that structural details such as the position of support and air-ducts, etc. (which were usually neglected in these methods) modify the calculation procedures to determine the natural frequencies. Furthermore, the motor structure has been changed due to the development of the manufacturing technology. For example, the casing and the stator are now usually press fitted together and are no longer coupled by key bars. Thus, previous theoretical models are no longer applicable. Since 1970s, Shumilov [20] and Yang [21] began to introduce the finite-element method for studying the vibration properties of motors and have shown that it gives more accurate results than previous analytical methods. The advantage of the finite-element method is that it can take into account the construction details of the motor structure, so that the effects of different parts of the structure can be investigated more accurately. However, as pointed out by Wang and Williams [22], because of the complexity of motor structures, up till now, no successful work on modelling the real motor structure has been reported.

In this paper, the vibration behaviour of a 2·2 kW induction motor structure is investigated using both experimental modal testing and finite-element modal analysis techniques. Five different experimental conditions are used to assess the influence of various structural parts such as the rotor, endshields and isolators on the vibration behaviour of the motor structure. Based on the experimental results obtained, the motor structure is modelled using the finite-element method. By comparing the calculated natural frequencies and mode shapes with the corresponding experimental results, appropriate models for each part of the motor structure are developed. The effects of the stator, casing, support and endshields on the vibration behaviour are discussed.

2. MODAL TESTING

2.1. EXPERIMENTAL SET-UP AND INSTRUMENTATION

The theory and procedures of modal testing are described in detail by Ewins [23]. A schematic diagram of the experimental set-up is shown in Figure 1. The equipment comprised a B&K type 2032 dual-channel FFT analyser, two B&K type 2635 charge amplifiers, and a B&K type 4383 accelerometer. Two kinds of excitations were used, namely random and impact excitation. For random excitation, a B&K type 4810 shaker driven by a B&K 2706 power amplifier was used to excite the motor casing via a B&K type 8001 impedance head. For impact excitation, a B&K 8202 hammer with a steel tip but without extra mass was used. The experimental data were acquired and analyzed using MODAL 3·0SE developed by SMS Inc. on a HP series 300 microcomputer. The frequency band of analysis was from 0 to 3·2 kHz.

The motor tested was a three-phase, 50 Hz, 2·2 kW induction motor manufactured by Fasco Australia. At rated output, the supply voltage, current and the speed are 415 V, 4·6 A and 1500 r.p.m. respectively. The motor structure is

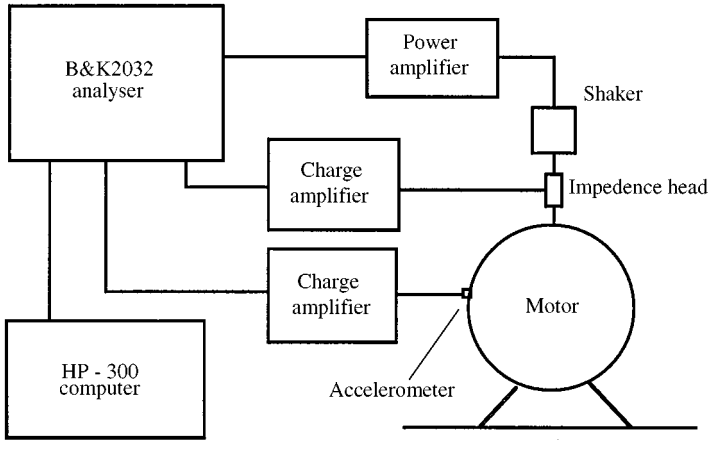

Figure 1. Schematic diagram of experimental set-up. Charge amplifier, B&K2635; power amplifier, B&K2706, shaker, B&K4810, impedance head, B&K8001; accelerometer, B&K4383.

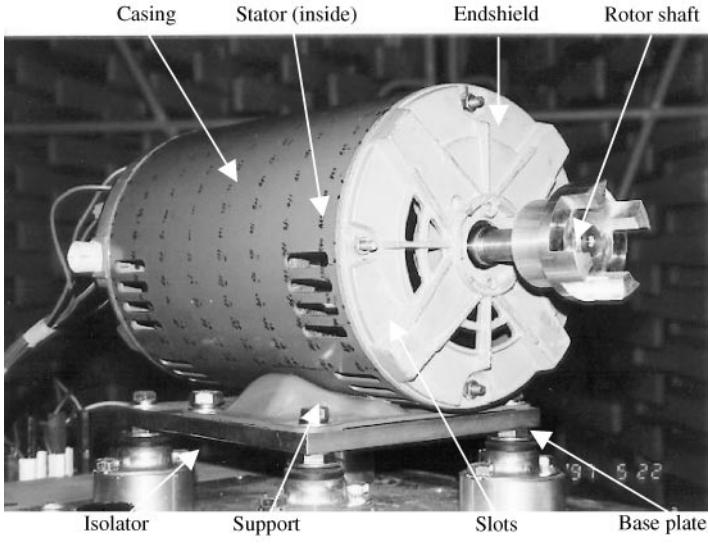

Figure 2. The test motor.

shown in Figure 2. As this motor is generally used with isolators, when tested with isolators it was resting on the test bench without any other treatment. But when tested without isolators, the motor with the support and the base plate was suspended by soft rubber bands, as shown in Figure 3. In this case, impact excitation had to be used because it was difficult to install the shaker properly. Considering the circumferential modes for the motor structure are usually more dominant than other modes, 31 measurement points on each of eight circumferences, giving a total of 248 points, were used, as shown in Figure 4(a). The excitation point for random excitation or the measurement point for impact excitation was No. 88 as shown in Figure 4(b).

In order to obtain a better understanding of the vibration modes of the motor and the effects of the rotor, the isolators, and end-shields, the following five experimental states were examined:

1. Point force random excitation in the radial direction—whole motor structure including rotor, isolators and end-shields.
2. Point force random excitation in the radial direction—without rotor but with isolators and end-shields.
3. Impact excitation in the radial direction—with rotor and end-shields but without isolators.
4. Impact excitation in the radial direction—without the rotor and isolators but with end-shields.
5. Impact excitation in the radial direction—without the rotor, isolators and the end-shields

As an electrical machine stator exhibits mainly a radial vibration behaviour [22], only the acceleration in the radial direction was measured in all the above experimental states.

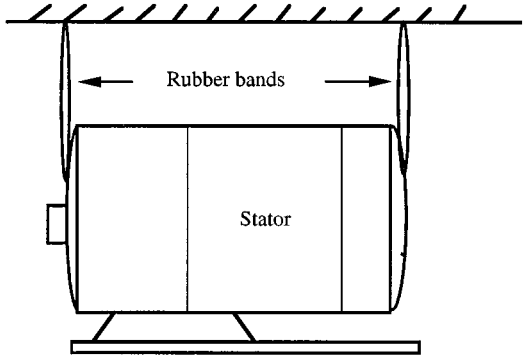

Figure 3. Test set-up of the motor without isolators.

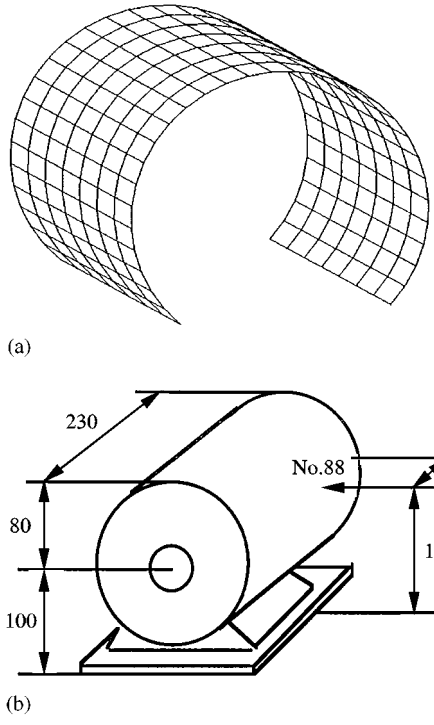

Figure 4. (a) The experimental measurement grid. (b) Geometry of the motor structure and measurement point. (dimensions are in mm)

2.2. MODAL TESTING RESULTS AND ANALYSIS

The modal testing results for the five experimental states are listed in Tables 1–5 respectively. By comparing the results of Tables 1 and 2, it can be found that mode 7, 11 and 15 which do not appear in Table 2 are due to the rotor. Furthermore, according to Figure 5 which shows the relative differences of the natural frequencies between states 1 and 2 against the mode number, it can be clearly seen that the

TABLE 1
Modal testing results of state 1

Mode number	Natural frequency (Hz)	Damping (%)	
1	8·54	14·2	Isolator
2	37·85	7·0	Isolator
3	119·71	4·2	Isolator
4	151·16	5·3	Isolator
5	210·49	4·8	Isolator
6	229·46	5·5	Isolator
7	294·47	1·4	Rotor
8	392·73	7·0	St./cas.
9	490·85	0·8	St./cas.
10	567·39	1·9	Seat
11	664·68	0·7	Rotor
12	717·67	1·6	Seat
13	770·00	0·3	Casing
14	816·52	0·4	Casing
15	928·30	0·9	Rotor
16	960·97	1·4	Casing
17	1057·27	0·7	Stator
18	1105·30	0·6	Stator
19	1240·70	0·8	Plate
20	1270·32	0·8	Casing
21	1307·18	1·2	Casing
22	1393·55	0·9	Seat
23	1480·60	1·0	Seat
24	1655·17	0·8	Casing
25	1743·04	0·9	Stator
26	1795·82	0·2	Stator
27	1869·31	0·5	Casing
28	1919·49	0·8	Casing
29	1988·05	0·3	Casing
30	2074·06	0·9	Casing
31	2176·77	0·8	
32	2244·57	0·9	
33	2335.83	0·9	
34	2446.46	1·6	

TABLE 2
Modal testing results of state 2

Mode number	Natural frequency (Hz)	Damping (%)
1	16·48	24·0
2	44·32	7·2
3	123·55	8·6
4	140·51	3·7
5	196·09	4·2
6	269·94	4·4
7		
8	373·47	3·0
9	476·76	1·8
10	562·20	0·4
11		
12	728·08*	1·6
13	713·48	0·6
14	844·97	2·5
15		
16	945·88	1·9
17	1049·90	0·8
18	1090·90	0·8
19	1235·10	1·2
20	1282·53	0·8
21	1305·00	0·1
22	1369·12	0·3
23	1467·50	0·9
24	1665·92	0·8
25	1695·83	0·8
26	1752·29	0·7
27	1866·74	0·3
28	1951·97	0·9
29		
30	2031·76	0·8
31	2163·54	0·6
32	2260·74	0·8
33	2349·49	0·3
34	2440·43	0·7

rotor appears to have a strong influence on the natural frequencies of modes 1, 2 and 6, but not very much on the modes of higher frequencies. This is because the first six modes are related to the isolators, and the change of the mass of the supported structure will change their natural frequencies. Note also that the boundary conditions of the motor stator and casing without the rotor are different from those with the rotor. According to the vibration theory of shells [24], higher order modes are not affected by the boundary conditions very much. Thus, the rotor should only affect the low-frequency modes. In fact, as the frequency increases, it is harder to find the modes caused by the rotor because the coupling

TABLE 3
Modal testing results of state 3

Mode number	Natural frequency (Hz)	Damping (%)	
1			
2			
3			
4			
5			
6			
7	283·46	1·0	Rotor
8	402·97	1·6	
9	473·06	0·8	
10	571·31	1·1	
11	638·73	0·8	Rotor
12	669·16	0·3	
13	763·56	0·3	
14	821·10	1·6	
15	892·86	1·0	Rotor
16	918·26	1·8	
17	1038·71	1·2	
18	1100·09	0·7	
19			
20	1179·91	0·7	
21	1282·55	1·3	
22	1425.05	0·7	
23	1551·45	0·6	
24	1639·72	0·5	
25	1720·61	0·8	
26	1743·96	0·6	
27	1855·91	1·2	
28	1930·65	0·3	
29	2030·18	0·2	
30	2061·14	0·5	
31	2206·97	1·7	
32	2277·46	1·3	
33	2338·50	1·1	
34	2449·32	0·2	

TABLE 4
Modal testing results of state 4

Mode number	Natural frequency (Hz)	Damping (%)
1		
2		
3		
4		
5		
6		
7		
8	404·28	0·7
9	584·40	1·2
10	668·39	0·1
11		
12	833·75*	2·2
13	736·68	0·8
14		
15		
16	966·83	0·5
17	1043·97	0·7
18	1097·55	0·7
19		
20	1179·73	0·5
21	1279·94	0·9
22	1418·64	0·5
23	1551·53	0·7
24	1636·95	0·9
25	1742·19	0·8
26	1723·14	0·3
27	1870·07	0·2
28	1924·96	0·3
29		
30	2041·52	0·7
31	2167·28	1·0
32	2239·56	0·7
33	2331·15	0·8
34	2423·58	0·8

between two connected structures at high frequencies is generally weaker than that at low frequencies. It was also reported by Zhu and Howe [13] that the rotor would introduce some new modes to the motor structure at low frequencies.

According to Tables 3 and 5 which show the results without the isolators, modes 1–6 related to the isolators cannot be determined. Modes 7, 11 and 15 still appear to be due to the rotor. Mode 19 which is not found in both states 3 and 4 might be due to the base plate. The relative differences between each frequency in Table 3 and that of the corresponding mode in Table 1 are within 5%. Thus, except for the modes caused by the isolators, all the other modes for the motor without isolators have

TABLE 5
Modal testing results of state 5

Mode	Experimental results	Causes of the mode	FEM results (model E)	FEM results (model E with teeth on the stator)
1	352·4		369·8	371·3
2	564·6		455·4	466·5
3	760·5		593·6	614·9
4	862·6	Stator (1,2)	748·6	780·9
5	929·2	Stator (1,2)	900·1	906·4
6	991·1	Stator (0,2)	991·2	954·5
7	1048·8	Stator (0,2)	1025·7	984·3
8	1149·8		1098·8	1100·0
9	1315·0		1303·8	1311·9
10	1368·8		1340·6	1359·6
11	1410·7		1381·9	1392·4
12	1459·1		1441·3	1444·9
13	1505·2		1449·4	1454·8
14	1559·0		1603·3	1602·7
15	1604·6		1605·6	1606·9
16	1683·3		1722·5	1732·6
17	1732·2		—	—
18	1843·3		1868·9	1840·2
19	1886·9		1891·7	1886·7
20	1966·4		1959·1	1956·6
21	2099·2		2049·3	2049·1

been determined with reasonable accuracy. This is because above the natural frequencies of the isolators, the motor with the isolators will behave as if free from the base support. Since the stiffness of each isolator has been determined to be $21{\cdot}8 \times 10^3$ N/m, the first natural frequency with the rotor theoretically is 10·8 Hz, which is reasonably close to the experimentally determined value of 8·54 Hz as given in Table 1.

It should be pointed out that in Table 1, all the vibration modes were numbered in the appearance order of modes in the frequency domain. For convenience of analysis, therefore, in Tables 2–4, all the modes are listed according to that number sequence by comparing the mode shapes of other states with those of state 1. Hence, in Tables 2 and 4 the mode marked with *, of which the frequency is higher than that of mode 13, was put in the position numbered 12. By arranging the modes in this fashion, and also by comparing the vibration modes of the first four experimental states, the main contributor to each vibration mode has been identified in Table 1. The modes considered to be related to the "seat", e.g. modes 10, 12 and 19, refer to those introduced by the support and the base plate, because the centre of gravity of the casing and the stator is vertically above the support points, as shown in Figure 3. Also "st./cas." refers to the case where the modes are caused by the stator mass and the stiffness of the casting, e.g., modes 8 and 9.

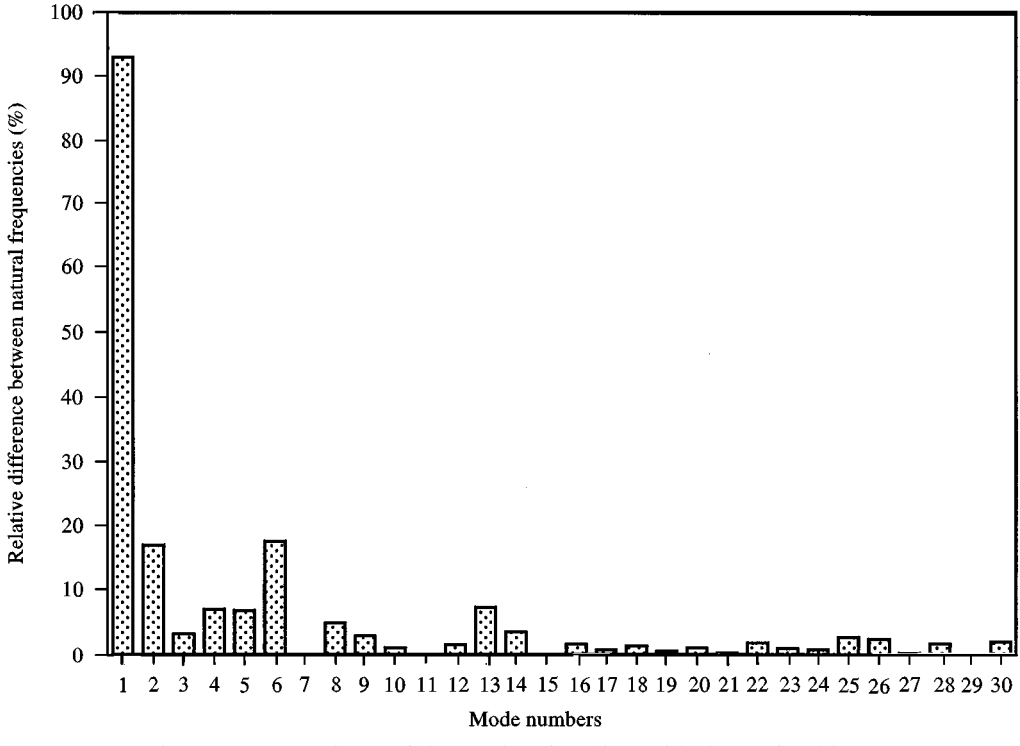

Figure 5. Comparisons of the results of Table 1 with those of Table 2.

Obviously, these vibration modes could be eliminated by simply changing its support structure, and adding some ribs to increase the stiffness of the casting in the axial direction.

In order to confirm the modal testing results, the structural modes identified in Tables 1 and 2 are marked in Figure 6 which displays three sound power spectra obtained from this motor driven by three inverters under no load condition [25]. It can be seen that almost corresponding to each peak in the sound power spectra, a vibration mode identified in Tables 1 and 2 can be found very close to it. These results indicate not only that the modal testing results obtained are reliable, but also that significant noise is caused by the coincidence between the harmonics of magnetic forces and structural natural frequencies. As the modes determined without the rotor are similar to those with the rotor as shown in Figure 6, experimental modal testing or numerical modelling may be conducted without the rotor if low-frequency modes are not of interest.

The purpose of considering state 5 is to examine the effects of end-shields on the vibration modes. In Table 5, 21 vibration modes are presented. In should be pointed out that all vibration modes here have to be renumbered because the absence of end-shields changes the boundary conditions of the motor casing so that their mode shapes are quite different from those in the previous four states. These modes, therefore, may have no direct relationship with those of the complete motor structure. However, for the motor structure considered here, as shown in Figure 7,

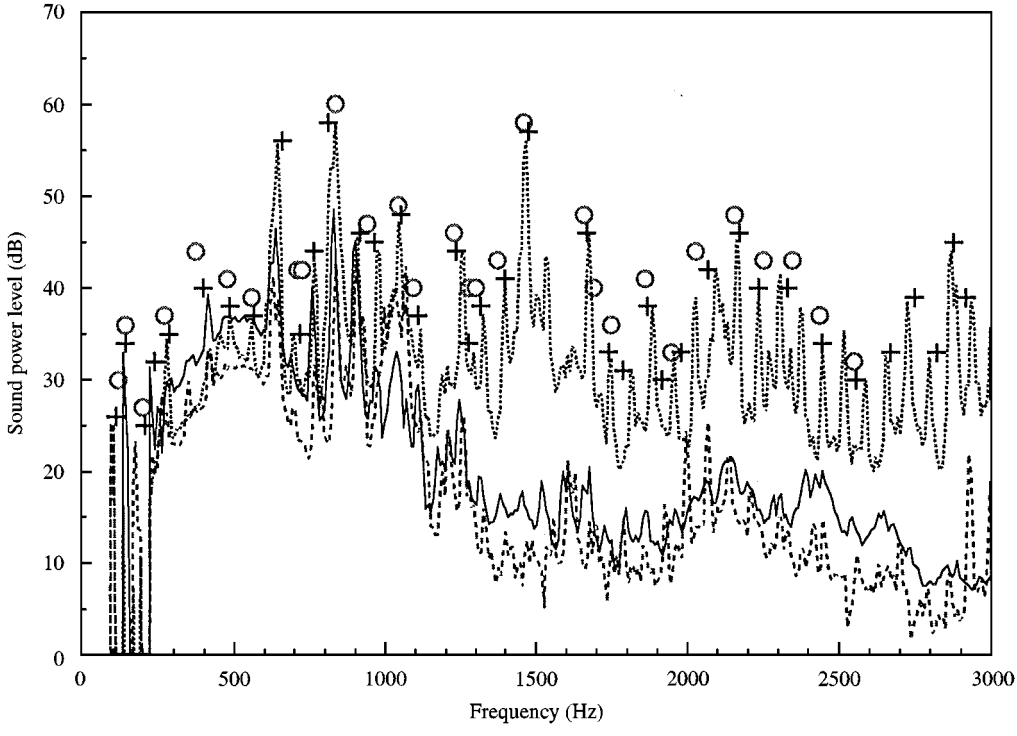

Figure 6. Sound power spectra and modal testing results of the motor: —— Benchmark, · · · · inverter 1, - - - - inverter 2, + Modal testing state 1, ○ Modal testing state 2

the stator is held in position with a uniform pressure applying from the casing on the outer surface of the stator. Therefore, the end-shields would affect the vibration behaviour of the stator through changing its load rather than changing its boundary conditions. As a result, the mode shapes of the stator should not be changed due to the absence of the end-shields except that their natural frequencies could change. Consequently, the modes caused by the stator are still comparable with the previous states. Actually, in Table 5, the modes 4 and 5 were found to correspond to the modes 25 and 26 in Tables 1–4, while modes 6 and 7 in Table 5 correspond to the modes 17 and 18 in the previous tables. It was also found that modes 4 and 5 in Table 5 or 25 and 26 in Table 1 are actually the (1, 2) mode of a cylindrical shell with the two ends free, and modes 6 and 7 in Table 5 or 17 and 18 in Table 1 are the (0, 2) mode. It is interesting to note that without end-shields, the frequencies of mode (1, 2) are lower than those of mode (0, 2), but with the end-shields, the frequencies of modes (1, 2) are higher. These results indicate that the end-shields have great influence on the vibration of the motor structure.

3. FINITE-ELEMENT MODELLING (FEM)

In order to investigate the effects of various substructures on the overall vibration behaviour of the motor structure, six models shown in Figure 8 which

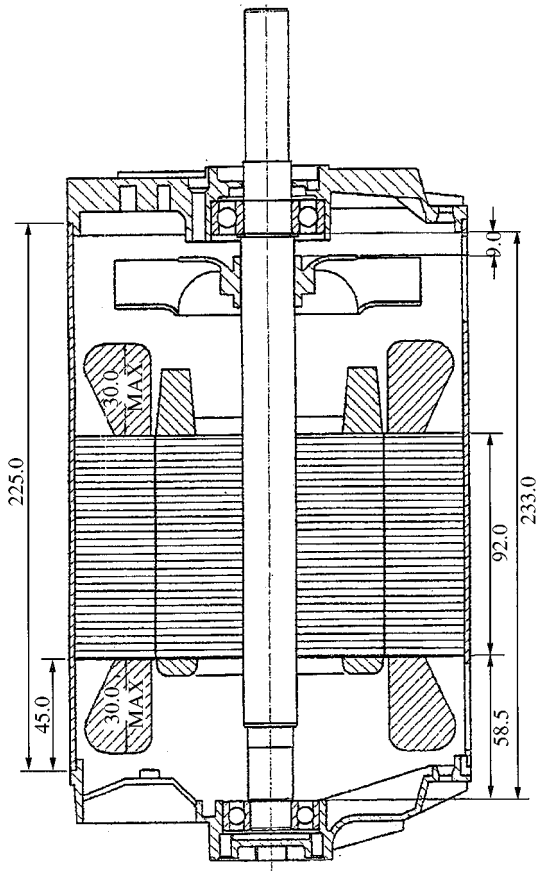

Figure 7. Geometry of the stator and the casing.

consider the teeth of the stator, casing, slots on the casing, support and end-shields in turn are developed. They are:

(A) the actual stator model [Figure 8(a)]
(B) a cylindrical shell stator model [Fig. 8(b)];
(C) a two cylindrical shell model of the motor [Fig. 8(c)];
(D) model C with the slots on the outer casing [Fig. 8(d)];
(E) model D with the support and the base plate [Fig. 8(e); and
(F) model E with end-shields [Fig. 8(f)].

3.1. MODELLING THE STATOR

The main part of the motor structure is the stator. Up till now many studies on its vibration and acoustic behaviour have been published [14–22, 26–29]. It is generally thought that, as far as the sound radiation from the motor structure is concerned, the radial vibration of the stator is the predominant noise source. Therefore, the analysis of the vibration characteristics of the stator is essential.

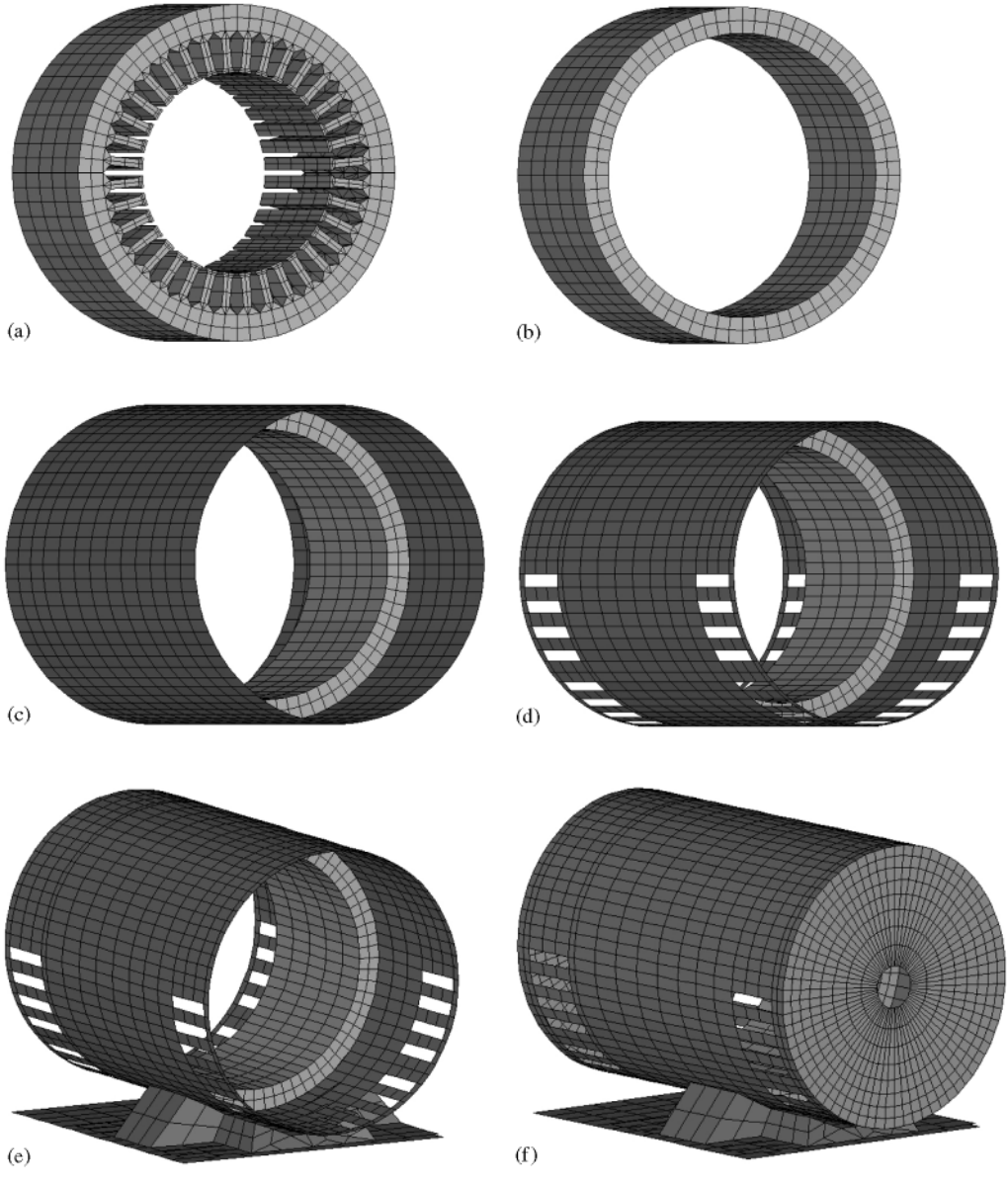

Figure 8. Finite element structural models: (a), the actual stator model; (b), a cylindrical shell stator model; (c), a two cylindrical shell model of the motor; (d), a two cylindrical shell model of the motor with slots on the outer casing; (e), a two cylindrical shell model of the motor with slots, the support and the base plate; (f), a two cylindrical shell model of the motor with slots, the support, the base plate and endshields.

The stator to be analyzed here is the same as that for the experimental modal testing. Figure 9 shows the geometry of the stator in details. It is a laminated steel stator, 0·092 m long with 36 teeth. The material density of each lamination is 7800 kg/m^3, and Young's modulus has been determined to be $13{\cdot}6 \times 10^{10}$ N/m^2 by

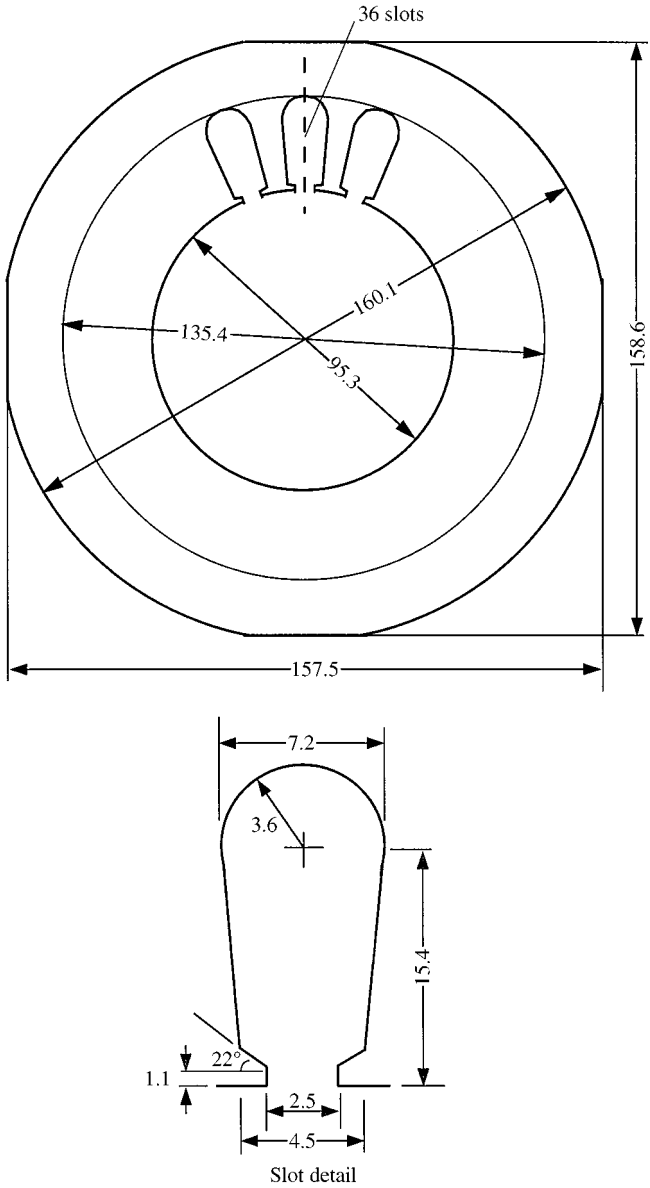

Figure 9. Geometry of the stator (dimensions are in mm).

using a dynamic method. The total masses of the stator and the windings are 6·6 and 2·88 kg respectively.

Calculations were made on a SUN SPARC20 workstation using a finite-element structural analysis software ANSYS (Revision 5·2) [30] developed by SASI. The material of the stator was first assumed to be isotropic. The element types were Brick eight-node Solid45 and Tetrahedron Solid72. A total of 3960 elements and 4104 nodes were used as shown in Figure 8(a). Since in the actual motor considered (see Figure 7) no constraints were applied at the two ends of the stator, the

TABLE 6
Natural frequencies of model A

Mode	Without windings	With windings	Mode order (m, n)* & type
1	1061·5	886·2	(0,2) S†
2	1062·4	886·9	(0,2) A
3	1842·6	1538·2	(1,2) S
4	1845·2	1540·4	(1,2) A
5	2802·4	2339·4	(0,3) S
6	2802.5	2339·5	(0,3) A
7	4052·0	3382·5	(1,3) S
8	4052·3	3382·8	(1,3) A

* m, n are the mode numbers in the axial and the circumferential directions respectively.
† S and A indicate symmetric and antisymmetric mode.

boundary conditions of the stator were set to be free at both ends. The subspace method was used for the modal analysis.

The first case considered was model A with and without windings. The windings were taken into account by treating them as an additional mass uniformly distributed in the stator. In ANSYS, this was done by changing the density of the material to 11193 kg/m^3. Table 6 lists the first 8 natural frequencies. It can be seen that the windings affect the natural frequencies of the stator very much. It can be deduced from Table 6 that an increase of the mass by 43·5% results in a reduction of the natural frequencies by 16·5%. These results indicate that the mass of the windings must be taken into account in developing a structural model with reasonable accuracy.

In order to investigate the effects of the teeth, the stator without teeth (i.e., a uniform cylindrical shell) was examined. As shown in Figure 8(b), the element type of model B was still Brick eight-node Solid 45, and there were a total of 1296 nodes and 720 elements (same as those in the non-teeth region of model A). Two cases, namely without windings and with windings, were also investigated. When windings were considered, because of a smaller volume of the model without teeth, the density was set to 13,293 kg/m^3 instead of 11,193 kg/m^3. Results in Table 7 show that, without windings, the teeth have a strong influence on the calculated natural frequencies. The difference varies from 1·3 to 18% for different modes. Note that the natural frequencies with teeth are lower than those without teeth. These results suggest that the mass of the teeth rather than stiffness is dominant so that the actual stator is under "mass control" above 1000 Hz. When the windings were considered, the differences between the two models became significantly smaller, less than 10% in general. This is because the total mass of the stator and windings (9·48 kg) is much greater than that of the teeth (2·5 kg), and consequently the vibration behaviour is dominated by the cylindrical shell. Therefore, when windings are considered, a cylindrical shell is a good approximate model to the stator being investigated. However, it should be emphasized that such an approximation may

TABLE 7
Natural frequencies of model B

Mode	Without windings	Difference between models A&B (%)	With windings	Difference between models A&B (%)	Mode order & type
1	1184·7	11·6	907·5	2·4	(0,2) S
2	1184·7	11·6	907·5	2·4	(0,2) A
3	1866·3	1.3	1429·6	7·1	(1,2) S
4	1866·3	1·3	1429·6	7·1	(1,2) A
5	3308·1	18·1	2534·0	8·3	(0,3) S
6	3308·1	18·1	2534·0	8·3	(0,3) A
7	4564·3	12·6	3496·3	3·4	(1,3) S
8	4564·3	12·6	3496·3	3·4	(1,3) A

not be valid for other stators, because it is possible that a stator with different number of teeth and geometry may have different behaviour.

3.2. MODELLING THE STATOR AND THE CASING

Like most other motor structures, the stator analyzed here is coupled with a thin steel frame which is also coupled with endshields, and support, as shown in Figure 7. Generally, this coupling will not only change the characteristics of the stator, but also those of the casing. However, Verma [27] discussed the effect of the outer frame tightly fitted over the periphery of the stator, and found that the coupling between the frame and the stator is "weak" and thus the frame could be neglected in the analysis. Note that for the motor of Verma [27], the mass of the frame was only 7% of the stator mass, Young's modulus of the frame was smaller than that of the stator, and its length in the axial direction was almost the same as that of the stator. The conclusion is reasonable. However, for the motor structure considered here, the density and Young's modulus of the material of the steel casing are 7800 kg/m^3 and $20{\cdot}6 \times 10^{10}$ N/m^2 respectively; the length of the casing is two times longer than that of the stator; and also the mass of the casing is about 20% of the stator mass. Verma's conclusions may not be applicable.

For simplicity, in ANSYS, a two cylindrical shell model which includes the mass of the windings in the stator was created (model C). Solid45 element type was used, and the total number of nodes and elements were 3120 and 1656 respectively, as shown in Figure 8(c). The mesh on each contact surface was the same, and the two shells were coupled by coupling the nodes on the contact surfaces in all degrees of freedom. The two ends of the casing were set to be free. Results obtained by assuming the material of the stator to be isotropic are listed in Table 8.

TABLE 8
Natural frequencies of models C and D

Mode	Model C with an isotropic stator	Model C with an orthotropic stator	Model D with an orthotropic stator	Experiment (state 5)	Mode order & type
1	1004·6	993·9	996·2	991·1	Stator (0,2) S
2	1004·6	994·7	996·7	1048·8	Stator (0,2) A
3	1158·6	758·3	776·8	862·6	Stator (1,2) S
4	1158·6	758·8	777·3	929·2	Stator (1,2) A
5	1531·0	1395·4	1280·5	1149·8	Casing
6	1531·0	1395·4	1339·9	1315·0	Casing
7	1634·7	1403·2	1397·1	1368·8	Casing
8	1634·7	1403·2	1434·2	1410·7	Casing
9	1780·3	1726·5	1557·0	1459·1	Casing
10	1780·3	1726·5	1571·8	1505·2	Casing

By comparing the results of model C with an isotropic stator (Table 8) with those of model B (Table 7), it can be seen that the vibration modes of the stator and casing are influenced by the coupling between the stator and the casing. For the casing, the vibration modes now are no longer those of the casing without the coupling. It can be conceived that the part of the casing attached to the stator would vibrate with the stator while the part not attached to the stator would not be constrained by the stator to move. For the stator, when the two ends of the casing are free, the first two natural frequencies are a little higher because the outer casing increases the stiffness of the stator. For the higher order modes of the stator, the outer casing seems to act as a mass load to the stator, thus decreasing the natural frequencies. Therefore, for small- and medium-sized motors of which the mass of the frame is not small compared with that of the stator, and the dimensions of the two structures are quite different, the outer frame of the stator can play an important role in the vibration and acoustic behaviour of the motor.

Note that model C shown in Figure 8(c) is similar to state 5 in the experimental modal testing. By comparing with results from the experimental modal testing in Table 8, it can be seen that except for the first mode caused by the stator, the frequencies of other modes are higher than those in the experiment. More importantly, for the modes caused by the stator, the calculated frequencies of modes (1, 2) are higher that those of modes (0, 2), whereas the measured frequencies of modes (1, 2) are lower. Although the differences between the natural frequencies of the modes (0, 2) and (1, 2) in calculation and experiment are within 10%, the opposite trend between calculations and experiments for these two modes should be further examined. Actually, for an isotropic cylindrical shell with both ends free, it is impossible for the frequency of (0, 2) mode to be higher than that of (1, 2) mode because the frequency of (0, 2) mode is the cut-off frequency for all vibration modes with $n = 2$ [31]. Note that the (1, 2) mode for a free–free cylindrical shell is one of

the inextensional modes which are mainly affected by the shear modulus in the cross-sectional plane, while the frequency of (0, 2) mode is mainly affected by Young's modulus in the circumferential direction [24, 32]. Therefore, it is possible that if the shear modulus in the cross-section plane is somehow small enough, the frequency of (1, 2) mode could be smaller than that of (0, 2) mode. This suggests that the material of the stator should be orthotropic rather than isotropic. Inspection of the motor structure reveals that the laminations are compressed in the axial direction as the radius of the motor casing is a little bit smaller than that of the stator laminations. Thus, although the density of the material of the stator remains at 7800 kg/m^3, the stiffness of the stator in the axial direction would not be the same as that of the stator made in solid material. It has been found that for a laminated structure like the stator here, Young's modulus in the axial direction is much smaller than that in the circumferential direction, and it also depends on the pressure acting in the axial direction [33]. As it is difficult to determine the pressure between the laminations in our case, according to Garvey [33], a typical value of Young's modulus in the axial direction, $2{\cdot}7 \times 10^9$ N/m^2 which is 2% of Young's modulus in the circumferential direction, was used. Results obtained for model C with an orthotropic stator are listed in Table 8. It can be seen that the order of the stator modes is now the same as that of the experiment. Furthermore, due to the reduction of the stiffness in the axial direction, the calculated frequencies of the casing modes approach those of the experimental results. These results suggest that it is essential to consider the material of the stator to be orthotropic.

3.3. MODELLING THE MOTOR STRUCTURE

Table 8 shows that even for model C with an orthotropic stator, the frequencies of casing modes are still higher than the experimental results. In order to improve the calculated frequencies further, the slots in the motor casing are modelled (model D). The slots are normally designed for ventilation. However, as these slots change not only the mass, but also the stiffness of the casing, the vibration properties of the casing, especially of the part extending over the stator, can change a lot. The calculated natural frequencies of model D are listed in Table 8. It can be seen that the frequencies of stator modes increase marginally, while the frequencies of casing modes decrease substantially. This is because, for the stator, the reduction in the casing mass decreases the load on the stator, and for the casing, the change of the stiffness dominates the effect.

By comparing the results of model D with an orthotropic stator in Table 8 with the experimental results in Table 5, it can be found that several experimental modes, for example modes 1–3, could not be determined by the calculations. In order to further improve on the predictions, a model shown in Figure 8(e) incorporating slots, the support and base plate was developed (model E). The support was fixed to the casing through eight points, and the base plate was fixed to the support through four points. The total number of nodes and elements are 3041 and 2127 respectively. Results obtained from this model (without teeth) are compared with those for the experimental state 5 in Table 5. For mode numbers

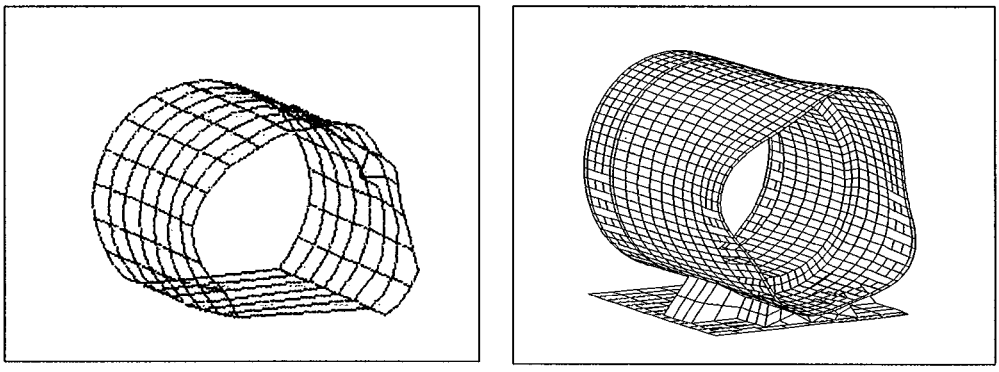

Mode 10 in Table 5

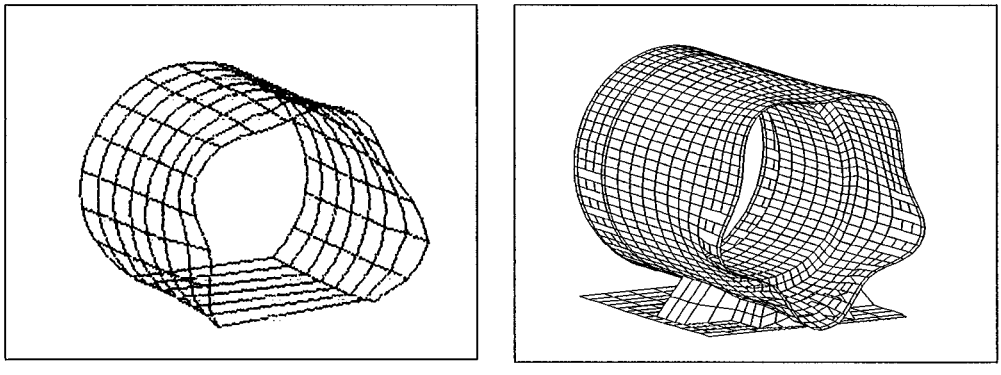

Mode 15 in Table 5

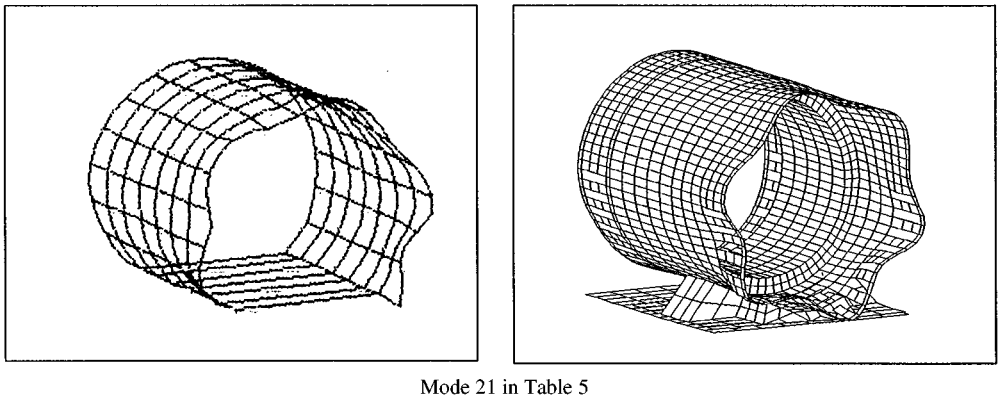

Mode 21 in Table 5

Figure 10. Comparison of calculated mode shapes (right hand side) with modal testing results (left hand side) of state 5.

greater than 4, the calculated natural frequencies and the mode shapes of the stator modes match the experimental results well. Also for each calculated mode which belongs to the casing or the support, these exists a corresponding mode in the experiment, as shown in Figure 10. By comparing Table 5 with Table 8, it can be seen that except for introducing several new modes, e.g. the modes 1–3 in Table 5, the inclusion of the support and the base plate reduces the frequencies of casing due

to-the increase of the effective mass of the casing. In order to examine the effect of the teeth of the stator, the stator teeth were added to model E, resulting in a total number of 6281 nodes and 5734 elements. The results are also listed in Table 5. Results of the two models (with and without teeth) are within 5% of each other, again indicating that for the motor structure considered here, the teeth of the stator may be neglected in the vibration analysis.

Finally, the end-shields are incorporated into the model (model F). The end-shields are made of aluminium by casting. As shown in Figure 2, the geometry of the end-shield is rather complex. However, the vibration of the end-shield itself may not be important. Since our interest is the influence of the end-shields on the vibration of the casing, instead of considering the detailed geometry of the end-shields, an equivalent end-shield in the form of a circular flat plate of the same mass, 0·36 kg, was considered. The thickness of the plate was chosen as 6 mm. The first natural frequency of the real end-shield was measured to be 1375 Hz by simply hitting the structure and examining the vibration spectrum. Young's modulus of the equivalent end-shield was determined to be 11×10^{10} N/m^2 by comparing the first natural frequency calculated by ANSYS with the experimental value of 1375 Hz. Therefore, a full model of the motor structure which includes the slots on the casing, support and the end-shields was created, as shown in Figure 8(f). The total number of nodes and elements are 4480 and 3423 respectively. The end-shields are coupled to the casing through coupling the corresponding nodes in all degrees of freedom. Results of calculated natural frequencies are compared with the experimental results of state 4 in Table 9. With the exception of several vibration modes at low frequencies that cannot be determined by the calculations, most of the vibration modes can be predicted. Figure 11 compares two of the calculated mode shapes with the experimental ones. Here the discrepancy between the prediction and the experiment seems to be larger than that presented in Table 5. This is because for a practical motor structure, the coupling between the endshields and the casing is rather complicated. For example, not all the points along the edges of the casing and end-shields are coupled; and also for those coupled points, their coupling strengths are different from each other. Obviously, all these details are too complex to be considered in the model. Nevertheless, for all the modes identified in the calculations, the natural frequencies are within 10% of the experimental values and may be acceptable as a model for acoustic prediction.

In order to further examine the effects of the support, base plate and the end-shields on the natural frequencies, two models which include the end-shields but without support and the base plate were examined (3144 elements and 4168 nodes) based on model F. Results listed in Table 9 indicate that when the support and slots are not modelled, in the frequency range of interest, only the modes caused by the stator can be found. When slots are considered, some vibration modes belonging to the casing then appear. These results therefore indicate that all the details of the motor structure, such as slots, support and base plate and end-shields affect the vibration behaviour of the motor very much.

It is worthwhile to emphasize here that the accuracy of the finite-element method depends on the element type and the number of elements and nodes used.

TABLE 9
Natural frequencies of model F

Mode number	Experimental results of state 4	FEM results (mode F)	FEM results (model F without support, and base plate)	FEM results (model F without slots, support and base plate)
1				
2				
3				
4				
5				
6				
7				
8	404·28	375·1		
9	584·40			
10	668·39	485·8		
11				
12	833·75*			
13	736·68	695·6		
14				
15				
16	966·83			
17	1043·97	1121·6	1109·6	1199·9
18	1097·55	1123·8	1135·0	1200·6
19				
20	1179·73	1097·5		
21	1279·94			
22	1418·64	1353·1		
23	1551·53	1559·6		
24	1636·95			
25	1742·19	1682·1	1733·6	2246·8
26	1723·14	1932·6	1909·9	2246·8
27	1870·07	1897·0		
28	1924·96			
29				
30	2041·52	2167·0	2468·7	
31	2167·28	2320·4	2536·5	
32	2239·56	2476·2	2708·0	
33	2331·15	2515·5	2785·4	
34	2423·58	2604·3	2848·2	

Generally, the more elements and nodes, the more accurate the results. However, too many elements require more computer memory and long computation time. In our analysis of a single cylindrical shell, the results were checked by doubling the elements and the nodes, and the difference between the results was less than 1%. Among all available element types, quadrilateral shape is the first choice.

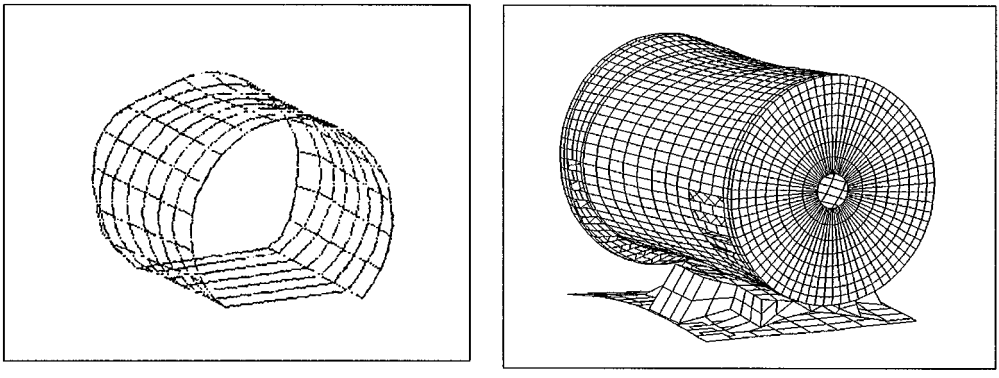

Mode 18 in Table 3

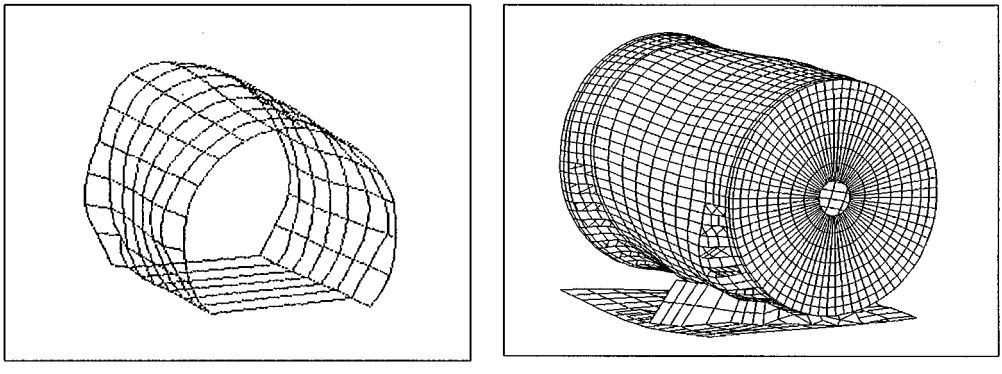

Mode 26 in Table 3

Figure 11. Comparison of calculated mode shapes with modal testing results of state 3.

4. CONCLUSIONS

The vibration characteristics of an induction motor have been investigated experimentally and using the finite-element modelling. The major conclusions are summarized below.

1. As the rotor is coupled to the motor casing through the end-shields, it would introduce some new vibration modes to the casing. However, this effect is only important at low frequencies. According to the theory, any change in the boundary conditions of a cylindrical shell, for example, the motor with or without the rotor, would not affect the vibration behaviour of the shell very much at high frequencies. Thus, if only the higher order modes due to the casing and stator are of interest, experimental modal testing may be conducted without the rotor.
2. As a motor is generally fixed to a support which imposes a boundary condition on the motor structure, modal testing should be conducted with the support. However, if there are isolators under the motor, when their natural frequencies are much lower than those of interest, tests can be conducted with the support free.

3. Since the end-shields actually determine the boundary conditions of the motor casing, they would significantly affect the vibration behaviour of the casing and the stator. Therefore, to obtain reasonable vibration modes of the motor, modal testing must be done with the end-shields.
4. In modelling a motor numerically, it is essential that the laminated stator must be modelled as an orthotropic structure in which Young's modulus in the axial direction is much smaller than that in the circumferential direction. As normally the exact value of Young's modulus in the axial direction is difficult to determine, 1–2% of that in the circumferential direction may be acceptable.
5. When modelling the stator, whether the teeth can be neglected or not depends on the balance of the effects of mass and stiffness on the natural frequencies. So care should be taken in modelling the stator as a uniform cylindrical shell. As windings generally contribute significantly to the mass of the motor, their mass should be taken into account.
6. When the mass percentage of the casing to the stator is not small and there are significant differences between the dimensions of the two in the axial direction, the outer casing cannot be neglected in the analysis. Also the slots on the casing would affect the natural frequencies of the stator and the casing because they not only change the mass, but also the stiffness of the casing.
7. The presence of the support would introduce some new vibration modes especially at low frequencies. At high frequencies, the effect of the support is to lower the natural frequencies of the casing because for the casing, the support acts like a mass load.
8. The end-shield affects the vibration behaviour of the casing because it changes the boundary conditions of the casing. Although generally it is rather difficult to model the coupling between the casing and the end-shields accurately, results obtained show that they may be considered to be coupled strongly.
9. Motor structures are complex. Basically, because each substructure would affect the overall vibration behaviour, all the structural details should be considered in the modelling, especially for small- and medium-sized motors for which the changes of the mass and stiffness due to the presence of slots and support are not negligible. Nevertheless, some simplifications in the modelling may be made. For the motor studied, the windings and the teeth are not modelled exactly but their mass is distributed uniformly throughout. Instead of modelling each lamina, the laminated stator is modelled as an orthotropic cylindrical shell structure. Also the end-shields are modelled as equivalent circular plates. Despite these simplifications, results obtained under these conditions are within 10% of the values determined from the experimental modal testing.

ACKNOWLEDGMENT

This project has been supported by the Australian Research Council. C. Wang acknowledges receipt of an Overseas Postgraduate Research Scholarship for the pursuit of this study.

REFERENCES

1. S. J. Yang 1981 *Low-noise Electrical Motors*. Oxford: Clarendon Press.
2. P. L. Timar 1988 *Noise and Vibration of Electrical Machines*. London: Springer-Verlag.
3. T. G. Habetler and D. M. Divan 1991 *IEEE Transactions on Power Electronics* **6**, 356–363. Acoustic noise reduction in sinusoidal PWM drives using a randomly modulated carrier.
4. A. Zuckerberger and A. Alexandrovitz 1986 *IEEE Transactions on Industrial Electronics* **IE-33**, 262–270. Determination of commutation sequence with a view to eliminating harmonics in microprocessor-controlled PWM voltage inverter.
5. P. N. Enjeti, P. D. Ziogas and J. F. Lindsay 1990 *IEEE Transactions on Industrial Applications* **26**, 302–316. Programmed PWM techniques to eliminate harmonics: a critical evaluation.
6. S. G. Otero and M. Devaney 1994 *IEEE Transactions on Industrial Applications* **30**, 111–115. Minimisation of acoustic noise in variable speed induction motors using a modified PWM drive.
7. P. L. Timar and J. C. S. Lai 1994 *Proceedings of IEE-Electric Power Applications*. **141**, 341–346. Acoustic noise of electromagnetic origin in an ideal frequency-converter-driven induction motor.
8. P. L. Timar, J. C. S. Lai and A. Illenyi 1994 *Proceedings of Inter-noise94, Japan*, 459–462. Does the ideal inverter eliminate the vibro-acoustic problems in variable-speed induction motor drives?
9. S. P. Verma and A. Balan 1993. *The 6th International Conference on Electrical Machines and Drives*, 546–551. Measurement techniques for vibration and acoustic noise of electrical machine.
10. S. P. Verma 1987 *The 3rd International Conference on Electrical Machines and Drives*, 113–117. Vibration behaviour of laminated stators of electrical machines.
11. R. Belmans and W. Geysen 1989 *Proceedings of EPE, Aachen*, 451–455. A case study of the electromechanical analysis of the audible noise in an inverter fed induction motor.
12. D. Verdyck, R. Belmans and W. Geysen 1991 *IEEE Transactions on Industrial Electronics* **27**, 539–544. Electro-mechanical analysis of the audible noise of an inverter-fed squirrel-cage induction motor.
13. Z. Q. Zhu and D. Howe 1989 *The 4th International Conference on Electrical Machines and Drives*, 232-236. Effects of end-shields and rotor on natural frequencies and modes of stator of small electrical machine.
14. J. P. Den Hartog 1928 *Transactions of American Society of Mechanical Engineers* **50**, 1–6 and 9–11. Vibration of frames of electrical machines.
15. H. Jordan and H. Frohne 1957 *Larmbekampfung* **1,** 137–140. Determination of resonance frequencies of stators of polyphase motors (in Germany).
16. H. Pavlovsky 1968 *Elektrotech. Obz.* **57**, 305–311. Vypocet vlastnich kmitoctu statorovych, svazku elektrickych stroju, elektrickych stroju.
17. S. P. Verma and R. S. Girgis 1975 *IEEE Transactions on PAS* **94**, 2151–2159. Considerations in the choice of main dimensions of stators of electrical machines in relation to their vibration characteristics.
18. E. Erdelyi 1955 *Ph.D. Thesis, University of Michigan*. Predetermination of the sound pressure levels of magnetic noise in medium induction motors.
19. A. J. Ellison and S. J. Yang 1971 *Proceedings of IEE* **118**, 185–190. Natural frequencies of stators of small electric machines.
20. J. A. Shumilov 1974 *Proceedings of the International Conference on Electrical Machines, London*. Calculating stator vibrations in electrical machines.
21. S. J. Yang 1978 *Proceedings of the International Conference on Electrical Machines, Brussels*. Finite element method in evaluating the stator natural frequencies of small machines.

22. H. Wang and K. Williams 1997 *Journal of Sound and Vibration* **202**, 703–715. Effects of laminations on the vibrational behaviour of electrical machine stators.
23. D. J. Ewins 1984 *Modal Testing: Theory and Practice*. Research Studies Press Ltd.
24. W. Soedel 1993 *Vibrations of Shells and Plates. New York*: Marcel Dekker, Inc., second edition.
25. D. Reyniers, J. C. S. Lai and D. Pulle 1996 *Inter-noise96, Liverpool*, 439–444. Acoustic studies of a 2·2 kW variable speed induction motor.
26. S. P. Verma and R. S. Girgis 1973 *IEEE Transactions on PAS* **92**, 1577–1585. Resonance frequencies of electrical machine stators having encased construction, Part I: derivation of the general frequency equation.
27. S. P. Verma and R. S. Girgis 1973 *IEEE Transactions on PAS* **92**, 1586–1593. Resonance frequencies of electrical machine stators having encased construction, Part II: numerical results and experimental verification.
28. S. P. Verma, K. Williams and R. K. Singal 1989 *Journal of Sound and Vibration* **129,** 1–13. Vibration of long and short laminated stators of electrical machines, Part I: theory, experimental models, procedure and setup.
29. K. Williams, R. K. Singal and S. P. Verma 1989 *Journal of Sound and Vibration* **129**, 15–29. Vibration of long and short laminated stators of electrical machines, Part II: results for long stators.
30. ANSYS User's Manual 1996 vision 5.2, ©SAS IP.
31. F. Fahy 1985 *Sound and Structural Vibration–Radiation, Transmission and Response*. London: Academic Press.
32. W. Leissa 1973 *NASA SP-288.* Washington, DC: *U.S. Government Printing Office*, Vibration of shells.
33. S. D. Garvey 1989 *The 4th International Conference on Electrical Machines and Drives*, 226–231. The vibrational behaviour of laminated component in electrical machine.